

International Journal of Automation and Control

ISSN online: 1740-7524 - ISSN print: 1740-7516

<https://www.inderscience.com/ijaac>

Frequency regulation of a time-delayed power system utilising a nonlinear resilient controller

Vivek Patel, Dipayan Guha, Shubhi Purwar

DOI: [10.1504/IJAAC.2024.10055534](https://doi.org/10.1504/IJAAC.2024.10055534)

Article History:

Received:	05 August 2022
Last revised:	24 January 2023
Accepted:	30 January 2023
Published online:	30 November 2023

Frequency regulation of a time-delayed power system utilising a nonlinear resilient controller

Vivek Patel*

Electrical Engineering Department,
Dr. Sakuntala Misra National Rehabilitation University,
Lucknow, India
Email: ree1702@mnnit.ac.in
*Corresponding author

Dipayan Guha and Shubhi Purwar

Electrical Engineering Department,
Motilal Nehru National Institute of Technology Allahabad,
Prayagraj, India
Email: dipayan@mnnit.ac.in
Email: shubhi@mnnit.ac.in

Abstract: In this work, an effort has been made to investigate the frequency regulation problem of a time-delayed interconnected power system (IPS) having redox flow battery (RFB). Frequency control is necessary for satisfactory output of power systems. An improved super twisting-based integral sliding mode controller (IST-ISMC) has been designed and incorporated in the IPS to actively compensate power-frequency oscillations in the wake of uncertain/unknown system disturbances. RFB has been introduced in the undertaken IPS because of high gain and smaller time constant, resulting in faster response. The stability of the closed-loop system has been affirmed by applying the Lyapunov-Krasovskii functional approach. Linear matrix inequality feasibility problem has been solved for designing the proposed controller. Simulation results show that IST-ISMC outperforms ISMC in terms of faster system dynamics, reduced chattering, and robustness against system uncertainty. The performance of the proposed controller is compared to the controller presented in Sun et al. (2018).

Keywords: frequency regulation; super twisting sliding mode controller; adaptive law; redox flow battery; RFB; linear matrix inequality; LMI.

Reference to this paper should be made as follows: Patel, V., Guha, D. and Purwar, S. (2024) 'Frequency regulation of a time-delayed power system utilising a nonlinear resilient controller', *Int. J. Automation and Control*, Vol. 18, No. 1, pp.87–109.

Biographical notes: Vivek Patel received his MTech degree from the Indian Institute of Technology (ISM) Dhanbad, Jharkhand, India. He is presently associated with the Electrical Engineering Department of Dr. Sakuntala Misra National Rehabilitation University, Lucknow, India. His research interests include stability and control of hybrid systems, nonlinear control, optimisation techniques, and estimation.

Dipayan Guha received his PhD in Electrical Engineering from the National Institute of Technology Durgapur, India. He is presently associated with the Electrical Engineering Department of Motilal Nehru National Institute of Technology Allahabad, Prayagraj, India. He has published 50 research papers in international journals and conference records. His research interests include nonlinear control, intelligent control, optimisation techniques, etc.

Shubhi Purwar received her BE from the VRCE, Nagpur, India, ME from MNREC, Allahabad, India, and PhD from Indian Institute of Technology Delhi, New Delhi, India, all in Electrical Engineering. She is currently a Professor with the Department of Electrical Engineering, MNNIT Allahabad. Her research interests include cyber-physical systems, stability and control of hybrid systems, nonlinear control, robotics, and intelligent control.

1 Introduction

In power system operation, the importance of frequency control problem is well known as it helps to attenuate the voltage and frequency oscillations caused by sudden variation load profiles. When the system is subjected to fast variations in load demands, the generators' input mechanical power is utilised to regulate the electrical output, i.e., frequency deviation (FD) and maintain the power flow between various control regions. As a result, a well-designed controlled power system should be able to handle the load fluctuations and system disturbances, while maintaining appropriate frequency and voltage (Ju et al., 1996).

Many physical systems contain time delays. These time delays affect system stability and may reduce system performance; thus, they should be appropriately considered in controller design (Muthana and Mohamed, 2013). Despite the fact that time delays exist in power system measurement and control loops, conventional power system controllers were often constructed primarily on local data and the time delays were often ignored. Wide-area measurement system method gives synchronised real-time measurements in the form of a phasor measurement unit, which may be utilised for power system stability investigations. This has led to interest in the area of measurement delay effects due to transmission channels. However to deal with this complex and challenging problem, requires the development of a more effective controller (Muthana and Mohamed, 2013).

1.1 Literature review and motivation

Many conventional and sophisticated strategies have been presented to tackle frequency regulation problems for single or interconnected power systems (IPSS). The proportional-integral (PI) control method was initially applied to solve load frequency control (LFC) problem (Sheirah and Abd-El-Fattah, 1984). A resilient proportional-integral-derivative (PID) control method for LFC of an IPS was investigated in Saxena and Hote (2016) and Lim et al. (1996). Optimisation-based LFC for IPS with parametric uncertainty is discussed in Gorripotu et al. (2018), Daneshfar and Bevrani (2012) and Jagatheesan et al. (2018). Optimal control (Arya et al., 2015), fuzzy logic (Sharma et al., 2020, 2021b; Arya and Kumar, 2016; Sudha and Santhi, 2011), and the LFC for a

nonlinear power system is studied in Guo and Dong (2017), Hussein et al. (2020) and Patel et al. (2021).

Time-delay is ignored in most of the literature (Bevrani et al., 2004) because they are mostly obtained from the local measurement device. Nevertheless, with the advancement of power systems, remote signals have become accessible as feedback signals in the design of advance power systems. As a result, time delay is becoming increasingly common, and they have become a source of system instability and degradation. For LFC of power systems with communication delays, two resilient, decentralised PI controller methods were presented in Bevrani and Hiyama (2008). Recently, fractional-order PID controller for LFC with time-delay is discussed in Kumar and Pan (2021). Yu and Tomsovic (2004) introduced a robust LFC approach based on linear matrix inequalities (LMIs). Jiang et al. (2012) studied the delay-dependent stability of an LFC method based on Lyapunov theory. Dey et al. (2012) examined the delay-based LFC problem and developed a two-term H_∞ controller based on LMIs. In Zhang et al. (2013), a delay-dependent robust approach for the study of a PID-based LFC with time delays was provided, along with an advanced method to measure robustness towards delays. The LFC problem is becoming increasingly important today, and some alternative impressive robust approaches should be investigated and established to provide rapid response, insensitivity to changes in system parameters, and minimum impacts of unmatched uncertainty.

Variable structure control has gained a lot of interest in the control community since the 1980s. Sliding mode control (SMC) is a type of variable structure control that is thought to be an effective way to cope with the system uncertainties of dynamical systems. Quick output response, easy implementation, insensitivity to fluctuation in system parameters, and total rejection of external disturbances are the key features of SMC (Utkin, 1977; Xia and Jia, 2003).

In Sun et al. (2018), H_∞ -based integral sliding mode control (ISMC) design for frequency regulation problem of IPS with time delay was investigated. H_∞ SMC with actuator saturation scheme for wind integrated power system and time delay is investigated in Pradhan and Das (2020). Nonlinear SMC has been utilised for two area power systems with communication delay, and is presented in Prasad et al. (2016). In Dev et al. (2021), the super twisting SMC approach for LFC in IPS with time delay is discussed.

Very few literature is available on time delay LFC problem. The advantages of SMC are well known. However, chattering (high-frequency oscillations) can be one of the major operational issues during the real-time implementation of the SMC. Chattering can lead to low control accuracy, increasing wear and tear of moving mechanical parts, and rise heat loss in actuators. As a result, an effective control scheme must be derived to improve system dynamics with significantly reduced chattering at the controller output.

In general, frequency and tie-line power oscillations persist for a long time when small load disturbances occur. Because of delayed response of governor system, it may not be able to absorb the frequency change in certain instances. In addition to the kinetic energy of the generator rotor, quick-acting energy storage systems (ESSs) can dampen electromechanical oscillations and offer storage capacity. The addition of energy storage units improves the power system's functioning (Kumar and Ganapathy, 2016; Heshmati et al., 2020). To stabilise load frequency difficulties in a two-area power system, superconducting magnetic energy sources (SMESs) are used in conjunction with a power electronic converter (Pappachen and Fathima, 2016). However, the large capital expenses

of the cooling units are the main drawback of a SMES. High power-rating capability, large energy storage capacity quick response time, and quick output response are all features of rechargeable batteries (Sharma et al., 2021a, 2021b; Dhandapani et al., 2018).

Given the preceding discussion, the following attributes motivates examining the present work:

- A very small time-delay might cause power system instability and deteriorate control performance of the time delayed power system, so it requires robust control techniques for frequency regulation problem of IPS in the presence of time-delay.
- SMC is an effective control strategy for designing controllers for time-delayed IPS because of its low sensitivity to changes in system parameters, finite-time convergence, quick response, and good control performance.
- Chattering (high-frequency oscillation) is a fundamental drawback of SMC, which can lead to the destruction of the final control element and leave the system more sensitive to instability. Therefore, while designing the SMC, chattering must be minimum without any loss in control accuracy.
- Due to the delayed response of the governor mechanism, controllers are unable to reduce FDs during high load disturbances in the areas of IPS. As a result, ESSs are installed in IPS due to their quick responses and for reimbursing deficient power in the dynamic conditions. They additionally minimise the grid FD and tie-line power deviation (T-LPD), consequently advancing the power quality.

1.2 Contributions

The key contributions of the present work are enumerated as follows:

- This article investigates the IPS with time delay and incorporates a fast-acting redox flow battery (RFB) in both the areas of IPS.
- Using the Lyapunov-Krasovskii (LK) functional approach to develop an improved stabilising criterion to satisfying H_∞ performance in the LMI framework.
- An improved super twisting-based integral sliding mode controller (IST-ISMC) is built to compensate the effect of time delays with reduced chattering phenomenon and to assure finite-time convergence of frequency and tie-line power variations under load disturbance.
- The consequences of inherent power system nonlinearities like generation rate constraints (GRC) and governor dead-band (GDB) on system outputs have been investigated.

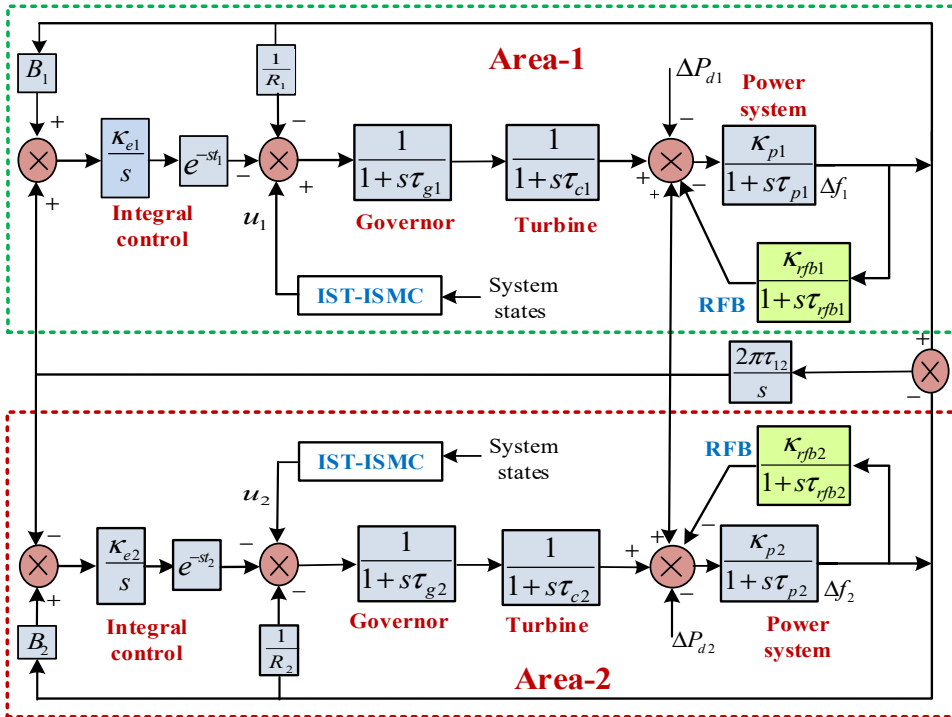
This paper makes a significant contribution by designing and applying an LMI-based IST-ISMC for investigating the frequency regulation problem of a time-delayed IPS with an RFB. An improved super twisting controller (ISTC) is an extension of the standard super twisting controller (STC), including an extra linear correction component to ensure convergence in finite time for a larger class of uncertainties with higher level of resilience and convergence speed. A constrained LMI optimisation problem is solved to compute the controller gain and optimal H_∞ performance index.

The remainder of the paper is laid out as follows. The frequency regulation problem for time delay power systems with the RFB model is explored in Section 2. In Section 3, a controller is developed, including time-delay in each area of IPS. In Section 4, simulation outcomes are provided to demonstrate the feasibility of the obtained results following the conclusions of work in Section 5.

2 System investigated

A linearised approach is appropriate for the frequency regulation problem since only small variations in load are envisaged during normal operation. For each area, there are governors, turbines, generators and loads. A super twisting-based ISMC technique for IPS with time-delay and RFB are investigated in this study.

Figure 1 Model of IPS with RFB (see online version for colours)



2.1 Two-area IPS with time-delay model

The dynamic equation of a two-area IPS with time-delay (in Figure 1) is provided to demonstrate the frequency regulation problem.

$$\Delta \dot{f}_i(t) = -\frac{1}{\tau_{pi}} \Delta f_i(t) + \frac{\kappa_{pi}}{\tau_{pi}} \Delta P_{gi}(t) - \frac{\kappa_{pi}}{\tau_{pi}} \Delta P_{ij}(t) - \frac{\kappa_{pi}}{\tau_{pi}} \Delta P_{di}(t) \quad (1)$$

$$\Delta \dot{P}_{ii}(t) = \left\{ -\Delta P_{ii}(t) + \Delta X_{gi}(t) \right\} \frac{1}{\tau_{ci}} \tag{2}$$

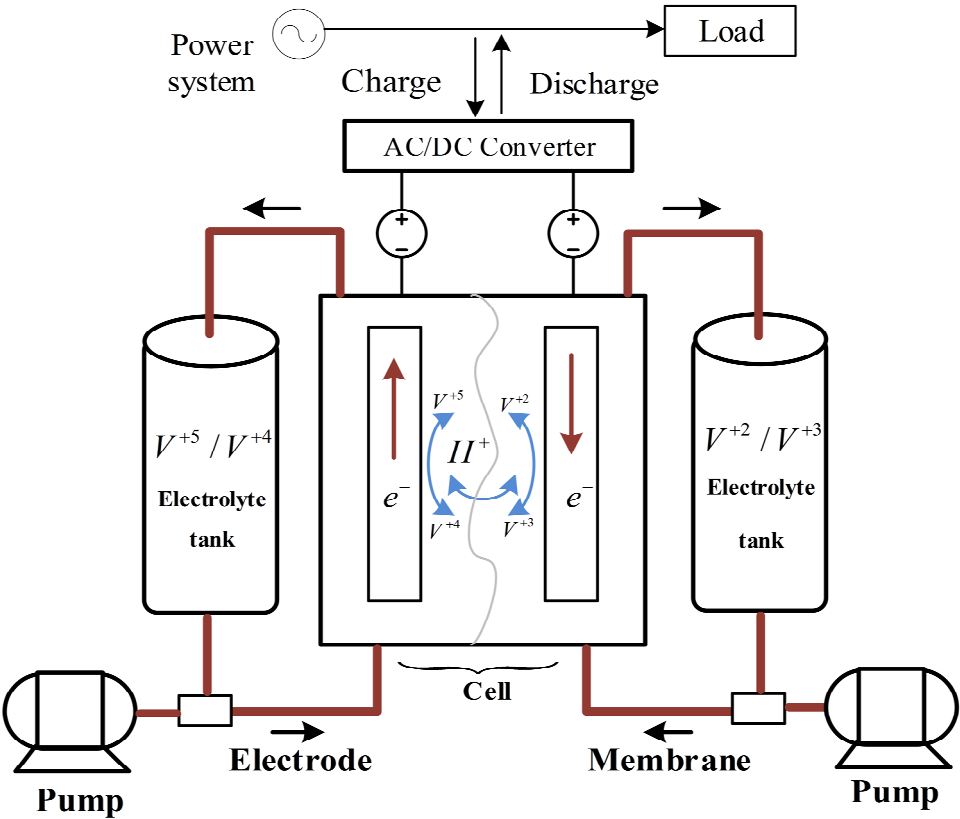
$$\Delta \dot{X}_{gi}(t) = -\frac{1}{R_i \tau_{gi}} \Delta f_i(t) - \frac{1}{\tau_{gi}} \Delta X_{gi}(t) - \frac{1}{\tau_{gi}} \Delta E_i(t - t_i) + \frac{1}{\tau_{gi}} u_i(t) \tag{3}$$

$$\Delta \dot{E}_i(t) = \kappa_{ei} B_i \Delta f_i(t) + \kappa_{ei} \Delta P_{tiej}(t) \tag{4}$$

$$\Delta \dot{P}_{tiej}(t) = 2\pi T_{i,j} (\Delta f_i(t) - \Delta f_j(t)) \quad \text{where } i, j = 1, 2 \text{ and } i \neq j \tag{5}$$

where Δf_i , ΔP_{ii} , ΔP_{tiej} , ΔX_{gi} and ΔE_i are the change in area frequency, non-reheat turbine output, tie-line interchange power, governor valve position, and integral control effort, in order; $\Delta P_{di}(t)$ is the deviation in the load demand, in order; τ_{gi} , τ_{pi} , τ_{ci} and τ_{12} are the time constants of speed governor, power system and turbine, and of tie-line interchange, in order.

Figure 2 RFB's working principle (see online version for colours)



Source: Dhandapani et al. (2018)

2.2 Operating principle of RFB

The RFB is an electrochemical system that utilises a reversible electrochemical action/operation to transfer electrical energy into chemical energy. The operating principles of an RFB are depicted in Figure 2. The vanadium ions (electrolytes) are dissolved in sulphuric acid (H_2SO_4) and kept in separate tanks before being supplied to the battery cell. The reaction of vanadium redox flow can be represented by equation (6), which is obtained by solving equations (7) and (8).



To maintain the charge balance in the cathode process, water (H_2O) and protons (H^+) are required. Easy maintenance, reduced deterioration, long-term storage, faster reaction, and no hunting are among the benefits of RFBs over conventional ESS (Dhandapani et al., 2018). To introduce high damping into power frequency oscillation against system disturbance, the output of RFB is utilised as compensating signal.

2.3 RFB model

The RFB's response is faster than that of the speed-governing system because it charges and discharges more frequently to reduce the oscillations in FDs when the load changes suddenly. Because it is quicker than the governor mechanism input, the RFB is treated as an active power source with time constant τ_{rfbi} and is presumed to be zero. Equation (10) gives the RFB transfer function model in terms of power change ΔP_{rfbi} . The IPS model with RFB model is depicted in Figure 1.

$$\frac{\Delta P_{rfbi}}{\Delta f_i} = \frac{\kappa_{rfbi}}{1 + s\tau_{rfbi}} \quad (9)$$

RFB's output response is much faster than the governor mechanism input. Hence, we assume $\tau_{rfbi} = 0$ (Dhandapani et al., 2018).

$$\Delta P_{rfbi} = \kappa_{rfbi} \Delta f_i. \quad (10)$$

2.4 Combine IPS with time delay and RFB model

The state space model of the overall investigated interconnected time-delay power system, is obtained as

$$\begin{aligned} \dot{x}(t) &= Ax(t) + A_{d1}x(t - t_{d1}) + A_{d2}x(t - t_{d2}) + Bu(t) + B_d d(t) \\ y(t) &= Cx(t) \end{aligned} \quad (11)$$

where $x(t)$, $u(t)$ and $d(t)$ are the states, control efforts, and disturbance input, in order. The matrices of equation (11) are obtained as.

$$A_{d2} = \begin{bmatrix} 0 & 0 & 0 & 0 & 0 & 0 & 0 & 0 & 0 & 0 \\ 0 & 0 & 0 & 0 & 0 & 0 & 0 & 0 & 0 & 0 \\ 0 & 0 & 0 & 0 & 0 & 0 & 0 & 0 & 0 & 0 \\ 0 & 0 & 0 & 0 & 0 & 0 & 0 & 0 & 0 & 0 \\ 0 & 0 & 0 & 0 & 0 & 0 & 0 & 0 & 0 & 0 \\ 0 & 0 & 0 & 0 & 0 & 0 & 0 & 0 & 0 & 0 \\ 0 & 0 & 0 & 0 & 0 & 0 & 0 & 0 & 0 & 0 \\ 0 & 0 & 0 & 0 & 0 & 0 & 0 & 0 & 0 & -\frac{1}{\tau_{g2}} \\ 0 & 0 & 0 & 0 & 0 & 0 & 0 & 0 & 0 & 0 \end{bmatrix}$$

Lemma 1 (Sun et al., 2018): Assuming a symmetric matrix $\Omega = \begin{bmatrix} \Omega_{11} & \Omega_{12} \\ \Omega_{21} & \Omega_{22} \end{bmatrix}$, where Ω_{11}

is $r \times r$ dimensional matrix, and $\Omega_{11} = \Omega_{11}^T$, $\Omega_{12} = \Omega_{21}^T$, $\Omega_{22} = \Omega_{22}^T$, the following are equivalents:

- 1 $\Omega < 0$
- 2 $\Omega_{11} < 0, \Omega_{22} - \Omega_{12}^T \Omega_{11}^{-1} \Omega_{12} < 0$
- 3 $\Omega_{22} < 0, \Omega_{11} - \Omega_{12}^T \Omega_{22}^{-1} \Omega_{12} < 0$.

3 Control strategy

The traditional SMC design consists of two separate parts: first is to identify the appropriate sliding surface for the desired output, and the second is to build the control law that will drive trajectory of the system to the sliding surface and keep it moving. In this work, time-delay is considered in both the areas of IPS.

3.1 Integral sliding surface

To enhance the system dynamics and resilience during the reaching phase, a modified PI type switching surface is defined as:

$$s(t) = \kappa_1 x(t) - \int_0^t \kappa_1 (A - B\kappa_2) x(\tau) d\tau - \int_0^{t-t_{d1}} \kappa_1 A_{d1} x(\tau) d\tau - \int_0^{t-t_{d2}} \kappa_1 A_{d2} x(\tau) d\tau \quad (12)$$

where κ_1 and κ_2 are control parameters, and κ_1 is chosen to guarantee matrix $\kappa_1 B \neq 0$. When the system dynamics reaches the sliding mode, the sliding surface defined in equation (12) satisfies the condition shown in equation (13).

$$s(t) = \dot{s}(t) = 0 \quad (13)$$

Differentiating equation (12) w.r.t. time, we have

$$\dot{s}(t) = \kappa_1 \dot{x}(t) - \kappa_1 (A - B\kappa_2) x(t) - \kappa_1 A_{d1} x(t - t_{d1}) - \kappa_1 A_{d2} x(t - t_{d2}) \quad (14)$$

From equation (11) and equation (14), we get

$$\dot{s}(t) = \kappa_1 B \kappa_2 x(t) + \kappa_1 B u(t) + \kappa_1 B_d d(t) \quad (15)$$

If the system trajectory fulfils $\dot{s}(t) = 0$, the equivalent control effort can be obtained as

$$u_e(t) = -\kappa_2 x(t) - (\kappa_1 B)^{-1} \kappa_1 B_d d(t) \quad (16)$$

The proposed control law $u(t)$ having two components $u_e(t)$ and $u_d(t)$.

$$\begin{aligned} u(t) &= u_e(t) + u_d(t) \\ \therefore u_e(t) \text{ and } u_d(t) &\text{ are the equivalent and discontinuous control law respectively.} \end{aligned} \quad (17)$$

Furthermore, by substituting equation (16) into system equation (11), the equivalent dynamic equation can be derived as

$$\left. \begin{aligned} \dot{x}(t) &= A_c x(t) + A_{d1} x(t - t_{d1}) + A_{d2} x(t - t_{d2}) + B_{dc} d(t) \\ z(t) &= Cx(t) \end{aligned} \right\} \quad (18)$$

The relationship between disturbance and output is

$$T_{dz}(s) = C [sI - (A_c + B\kappa_1) - A_{d1} e^{-t_{d1}s} - A_{d2} e^{-t_{d2}s}] B_{dc} \quad (19)$$

The controller is designed to satisfy the H_∞ norm condition.

$$\|T_{dz}(s)\|_\infty < \gamma, \gamma > 0. \quad (20)$$

Note 1: In contrast to the conventional switching surface design methods (Mi et al., 2013), which only consider the proportional and integral parts, the main objective of this paper to consider time-delay between the control areas while designing switching surface. Therefore, two integral parts with appropriate time-delays have been included to the switching surface function.

3.2 Stabilisation criterion

Stabilising criteria is presented in the LMI framework in the following theorem.

Theorem 1: The system equation (18) is asymptotically stable with $\|T_{dz}(s)\|_\infty < \gamma$, ($\therefore \gamma > 0$), for $t_{d1} > 0$, $t_{d2} > 0$, if there exist matrices such that $P^T = P \in \mathbb{R}^{n \times n}$, $0 < Q_1 < Q_1^T = Q_1 \in \mathbb{R}^{n \times n}$, $0 < Q_2 < Q_2^T = Q_2 \in \mathbb{R}^{n \times n}$ as well as matrix Ω that satisfies the following LMI:

$$J = \left. \begin{array}{ccccc} \varphi_{11} & PC^T & A_{d1}P & A_{d2}P & B_d \\ * & -I & 0 & 0 & 0 \\ * & * & -Q_1 & 0 & 0 \\ * & * & * & -Q_2 & 0 \\ * & * & * & * & \gamma^2 I \end{array} \right\} \quad (21)$$

$$J < 0, \varphi_{11} = AP + PA^T + B\Omega + \Omega^T B^T + Q_1 + Q_2$$

Furthermore, the state feedback controller's gain can be computed by

$$\kappa_2 = \Omega P^{-1}. \quad (22)$$

Proof: In the beginning, develop the following L-K functional for the stability of the controlled IPS [equation (18)] with $d(t) = 0$:

$$v(t) = x^T(t)Px(t) + \int_{t-t_1}^t x^T(s)Q_1x(s)ds + \int_{t-t_2}^t x^T(s)Q_2x(s)ds \quad (23)$$

The derivative of equation (23) is calculated along the system [equation (18)], one can obtain

$$\begin{aligned} \dot{v}(t) = & \dot{x}^T(t)Px(t) + x^T(t)P\dot{x}(t) + x^T(t)(Q_1 + Q_2)x(t) - x^T(t-t_1)Q_1x(t) \\ & - x^T(t)Q_2x(t-t_2) \end{aligned} \quad (24)$$

$$\dot{v}(t) = \phi^T(t)\Psi\phi(t) \quad (25)$$

$$\phi(t) = [x^T(t), x^T(t-t_1), x^T(t-t_2)]^T \quad (26)$$

$$\Psi = \left. \begin{array}{ccc} A_c^T P + PA_c + Q_1 + Q_2 & PA_{d1} & PA_{d2} \\ * & -Q_1 & 0 \\ * & * & -Q_2 \end{array} \right\} \quad (27)$$

$$\therefore A_c = A - B\kappa_2$$

Using Lemma 1, we may conclude from the LMI criterion equation (21) that $\Psi < 0$, which means $\dot{v}(t) < 0$. Hence, it can be concluded that the frequency of system [equation (18)] is asymptotically stable with $d(t) = 0$.

Moreover, define the following performance index with a defined attenuation level $\gamma > 0$:

$$J_{zd} = \int_0^{\infty} [\gamma^{-1}z^T z - \gamma d^T d] dt \quad (28)$$

If $J_{zd} \leq 0$, then system equation (18) is robustly stable and fulfils the condition $H_{\infty} \leq \gamma$. Therefore, the next objective is to prove that $J_{zd} \leq 0$. For zero initial condition $u(0) = 0$ and since $u(\infty) \geq 0$, one can get

$$\left. \begin{aligned} J_{zd} &\leq \int_0^{\infty} [\gamma^{-1} z^T z - \gamma d^T d + \dot{v}(t)] dt \\ &= \int_0^{\infty} \Theta^T(t) \Delta \Theta(t) dt \end{aligned} \right\} \tag{29}$$

$$\therefore \Theta(t) = [x^T(t), x^T(t-t_1), x^T(t-t_1), d^T(t)] \tag{30}$$

$$\Delta = \begin{bmatrix} A_c^T P + P A_c + Q_1 + Q_2 + \gamma^{-1} C^T C & P A_1 & P A_2 & P B_{d_c} \\ * & -Q_1 & 0 & 0 \\ * & * & -Q_2 & 0 \\ * & * & * & -\gamma I \end{bmatrix} \tag{31}$$

We can ensure that the system equation (18) is robustly stable by applying Lemma 1, which follows the condition equation (21) that $\Delta < 0$, since we know $J_{zd} \leq 0$.

Moreover, the optimal attenuation level can be determined by solving the ensuing constrained optimisation problem:

$$\left. \begin{aligned} \min_{t_1, t_2, P, Q_1, Q_2, \Omega} \eta \\ \text{s.t. } P > 0, Q_1 > 0, Q_2 > 0, J < 0 \end{aligned} \right\} \tag{32}$$

where γ can be determined by $\gamma = \sqrt{n}$.

Note 2: Theorem 1 could guarantee that the system equation (18) with disturbance is stable and resilient with the best attenuation level γ based on the proposed control approach.

3.3 Design of STC

The STC is also known as a second-order SMC. It has distinctive features, such as chattering attenuation, while maintaining robustness. The STC is a continuous controller to ensure all first order SMC’s main properties for the system with bounded matched uncertainties (Akbar and Uchiyama, 2018). For the dynamic system [equation (18)], the super twisting switching control law is defined as

$$\left. \begin{aligned} \dot{s}(t) &= -\kappa_a \|s(t)\|^{0.5} \text{sign}(s(t)) + c_{st} \\ \dot{c}_{st} &= -0.5\kappa_b \text{sign}(s(t)) \end{aligned} \right\} \tag{33}$$

The control equation (33) ensures the finite time convergence (Akbar and Uchiyama, 2018). This algorithm has a key property that allows it to be directly applied to systems with a relative degree of one.

From equation (33), we can obtain a control law u_{st} in equation (34)

$$u_{st} = -\kappa_a \|s(t)\|^{0.5} \text{sign}(s(t)) - \int_0^t 0.5\kappa_b \text{sign}(s(t)) dt. \tag{34}$$

3.4 Improved super twisting controller

The improved super twisting algorithm adds an extra linear correction term to the standard STC with a proportional plus constant and power rate reaching law, ensuring convergence in finite time for a broader class of uncertainties. It has a higher level of resilience as well as a faster rate of convergence (Akbar and Uchiyama, 2018, 2017). The sliding dynamics is

$$\left. \begin{aligned} \dot{s}(t) &= -\kappa_x \Xi_1 + c_{st} \\ \dot{c}_{st} &= -\kappa_y \Xi_2 \end{aligned} \right\} \quad (35)$$

where

$$\left. \begin{aligned} \Xi_1 &= \Lambda_1 \|s(t)\|^{0.5} \text{sign}(s(t)) + \Lambda_2 s(t) \\ \Xi_2 &= \frac{3}{2} \Lambda_1^2 \text{sign}(s(t)) + \Lambda_1 \|s(t)\|^{0.5} \text{sign}(s(t)) + \Lambda_2^2 s(t) \end{aligned} \right\} \quad (36)$$

are the nonlinear stabilising terms and $\Lambda_1, \Lambda_2 > 0$. We choose that $\Lambda_1 = 1$ and assume and $\Lambda_2 = k_z (> 0)$, then equation (36) becomes

$$\left. \begin{aligned} \Xi_1 &= k_z \|s(t)\|^{0.5} \text{sign}(s(t)) + s(t) \\ \Xi_2 &= \frac{3}{2} k_z^2 \text{sign}(s(t)) + \frac{1}{2} k_z \|s(t)\|^{0.5} \text{sign}(s(t)) + s(t) \end{aligned} \right\} \quad (37)$$

From equation (35), we can obtain a switching control law in equation (38)

$$\begin{aligned} u_{st} &= -\kappa_x \left\{ s(t) + k_z \|s(t)\|^{0.5} \text{sign}(s(t)) \right\} \\ &\quad -\kappa_y \int_0^t \left\{ s(t) + \frac{3}{2} k_z^2 \text{sign}(s(t)) + k_z \|s(t)\|^{0.5} \text{sign}(s(t)) \right\} dt \end{aligned} \quad (38)$$

where $\kappa_x, \kappa_y > 0$ are constant, which is given in Appendix.

We use gain adaptive law (Akbar and Uchiyama, 2018) in the study, since the upper bound on $d(t)$ in equation (16) is unknown.

$$\dot{\kappa}_x = \begin{cases} \bar{k}_x \sqrt{\frac{\gamma_x}{2}} \text{sign}\{s(t) - \mu_x\} & \text{if } \kappa_x > \kappa_m (= 0.01) \\ \eta_i & \text{if } \kappa_x \leq \kappa_m \end{cases} \quad (39)$$

$$\kappa_y = 2\epsilon \kappa_x \quad (40)$$

Final control law of IST-ISMC is defined as

$$u = u_{st} + u_e \quad (41)$$

$$u = -\kappa_2 x(t) - (\kappa_1 B)^{-1} \kappa_1 B_d d(t) - \kappa_x \left\{ s(t) + \kappa_z \|s(t)\|^{0.5} \text{sign}(s(t)) \right\} - \kappa_y \int_0^t \left\{ s(t) + \frac{3}{2} \kappa_z^2 \text{sign}(s(t)) + \kappa_z \|s(t)\|^{0.5} \text{sign}(s(t)) \right\} dt \quad (42)$$

where $\gamma_x, \varepsilon, \bar{\kappa}_x, \eta$ and κ_m are positive constants, μ_x is a positive parameter that defines the boundary layer for the sliding mode. Under a few assumptions in Akbar and Uchiyama (2018), the STC with adaptive gains equations (39)–(40) attains the finite-time convergence to a second order-sliding mode when $|s(t)| \leq \bar{\omega}$ and $\bar{\omega} \geq \mu_x$.

3.5 Stability analysis

Considering a candidate Lyapunov function as

$$v(t) = 0.5 s^T(t) s(t) \quad (43)$$

$$\begin{aligned} \dot{v}(t) &= 0.5 \dot{s}^T(t) s(t) + 0.5 s^T(t) \dot{s}(t) \\ &= s^T(t) \dot{s}(t) \end{aligned} \quad (44)$$

$$\dot{v}(t) = s^T(t) [\kappa_1 B \kappa_2 x(t) + \kappa_1 B u(t) + \kappa_1 B_d d(t)] \quad (45)$$

$$\begin{aligned} \dot{v}(t) &= \\ s^T(t) &\left[\kappa_1 B \kappa_2 x(t) + \kappa_1 B \left\{ -\kappa_2 x(t) - (\kappa_1 B)^{-1} \kappa_1 B_d d(t) - \kappa_x \left\{ s(t) + \|s(t)\|^{0.5} \text{sign}(s(t)) \right\} \right\} \right] \end{aligned} \quad (46)$$

$$\begin{aligned} & - \kappa_y \int_0^t \left\{ s(t) + \frac{3}{2} \kappa_z \text{sign}(s(t)) + \kappa_z \|s(t)\|^{0.5} \text{sign}(s(t)) \right\} dt \Big] + \kappa_1 B_d d(t) \\ \dot{v}(t) &= s^T(t) \left[\kappa_1 B \left\{ -\kappa_x \left(s(t) + \|s(t)\|^{0.5} \text{sign}(s(t)) \right) \right. \right. \\ & \left. \left. - \kappa_y \int_0^t \left\{ s(t) + \frac{3}{2} \kappa_z \text{sign}(s(t)) + \kappa_z \|s(t)\|^{0.5} \text{sign}(s(t)) \right\} dt \right\} \right] \end{aligned} \quad (47)$$

From equation (47), $\dot{v}(t) < 0$ can be confirmed that the system is asymptotically stable with proper choice of $\kappa_1, \kappa_x, \kappa_y$ and κ_z using control law equation (42).

4 Simulation results

The simulation was conducted under different operating scenarios was conducted to assess the performance of IST-ISMC in frequency regulation of IPS with time-delay. The designed controller's competence is verified by comparison with existing literature results in terms of FD, peak overshoot, speed of response and damping of oscillation. The

simulation was run on MATLAB R2018a domain. For evaluating the efficacy of the designed controller, the following cases were considered.

Case 1

In this case, a load perturbations, i.e., $\Delta P_{d1} = 0.1$ pu and $\Delta P_{d2} = 0.1$ pu at $t = 10$ s, and 0.1 pu initial condition [for fair comparison with ISMC (Sun et al., 2018)] are applied simultaneously to the IPS (without RFB integrated). The FD, T-LPD, and control inputs (CIs) are shown and compared with ISMC (Sun et al., 2018) in Figure 3. It is seeming from Figures 3(a)–3(c) that the suggested IST-ISM speeds up the responses of the system with smaller undershoot (US)/overshoot (OS) and small setting time compared to ISMC (Sun et al., 2018).

The chattering problem is the most difficult aspect of SMC design. Chattering in a plant can result in poor control efficiency, loud noise and excessive heat losses. The CI adjusts the governor valves (actuator) position to control the entry of steam into the turbine blades, and reducing governor valve tear and wear problem in the steam turbine servo system. The suggested IST-ISM design also minimised chattering in CI without reducing response speed, as shown in Figures 3(d)–3(e).

Figure 3 (a) FD in area-1 (b) FD in area-2 (c) T-LPD (d) CI in area-1 (e) CI in area-2 (see online version for colours)

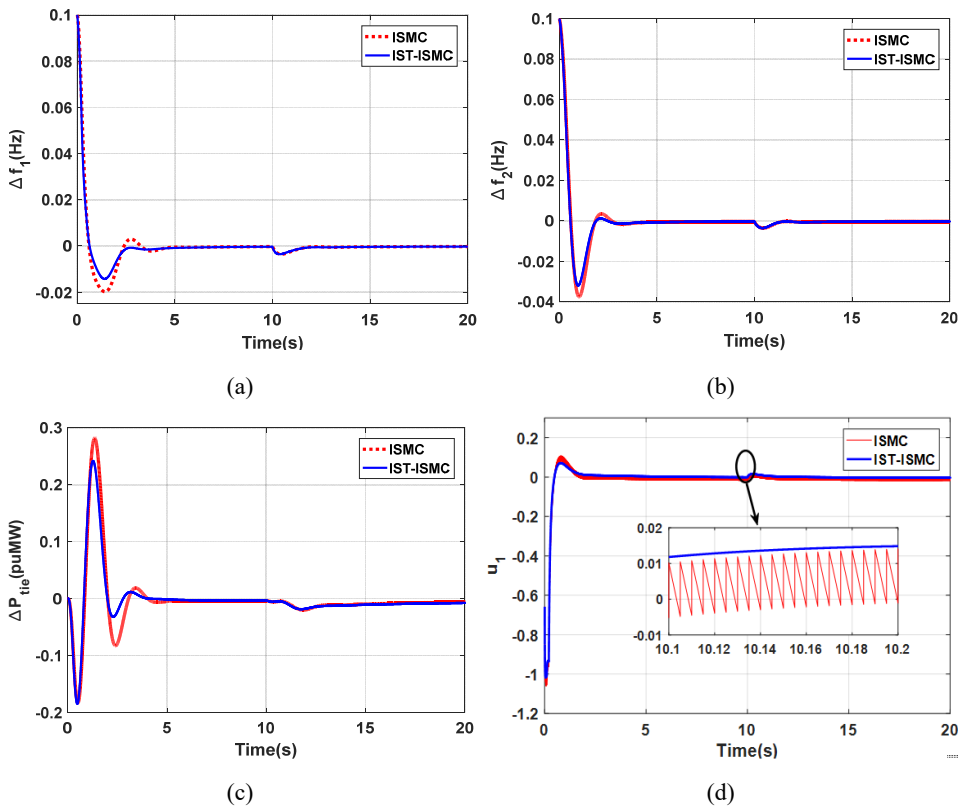


Figure 3 (a) FD in area-1 (b) FD in area-2 (c) T-LPD (d) CI in area-1 (e) CI in area-2 (continued) (see online version for colours)

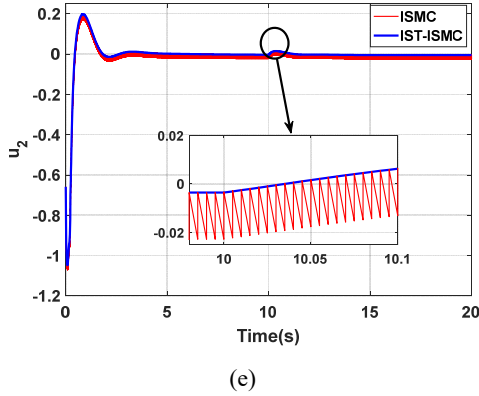


Figure 4 (a) FD in area-1 (b) FD in area-2 (c) T_LPD (d) CI in area-1 (e) CI in area-2 (see online version for colours)

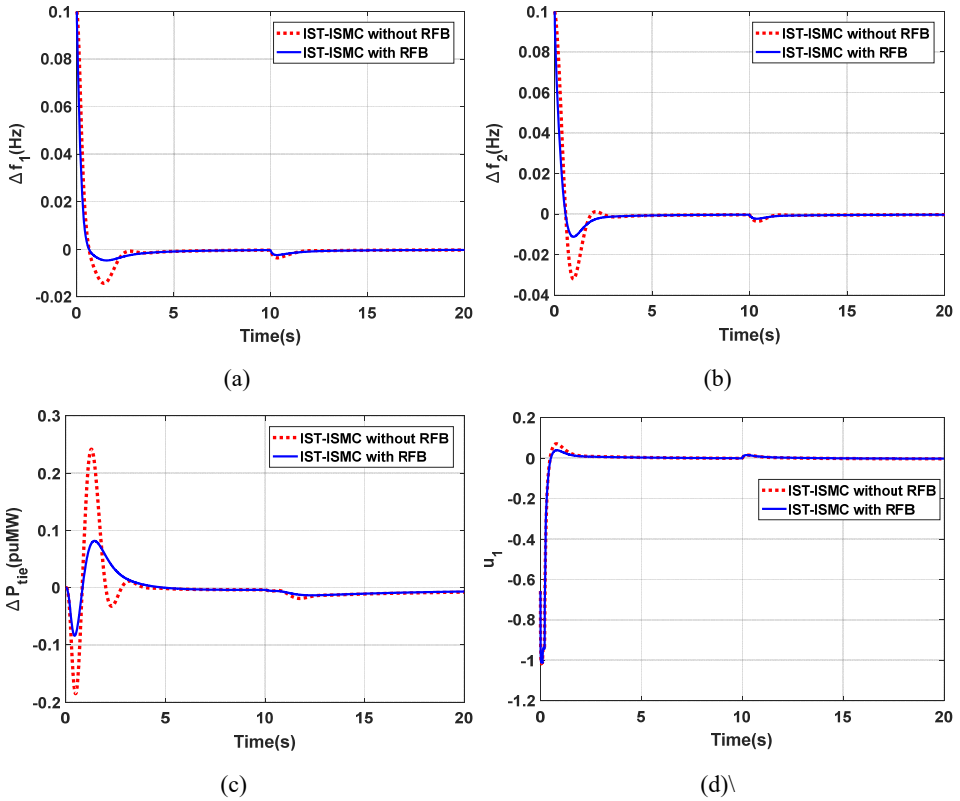
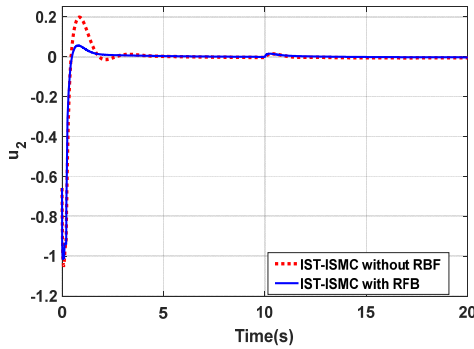


Figure 4 (a) FD in area-1 (b) FD in area-2 (c) T_LPD (d) CI in area-1 (e) CI in area-2 (see online version for colours)



(e)

Case 2

In this case, load perturbations, i.e., $\Delta P_{d1} = 0.1$ pu and $\Delta P_{d2} = 0.1$ pu at $t = 10$ s, are applied simultaneously to IPS (with RFB integrated) to illustrate the ability of IST-ISM with RFB on the T-LPD and FD. It is seen from Figures 4(a)–4(c) that the FD and T-LPD with the applied IST-ISM with RFB is significantly improved compared to IST-ISM without RFB. The magnitude of peak OS and US is observed to be minimised when RFB is provided in both the areas, it also significantly minimises the system oscillation. The CI plots are given in Figures 4(d)–4(e).

Case 3

The dynamic performance of IPS with RFB is further investigated including GDB nonlinearity with GRC (in Figure 5) to highlight the possible benefits of employing IST-ISM, and the results are shown in Figure 6. The GDB and GRC’s limiting values selected for simulation are ± 0.0006 (Prasad et al., 2016) and ± 0.0006 pu MW/sec (Prasad et al., 2016), respectively. The US/peak OS rises after GRC and GDB are added to the system, as seen in Figures 6(a)–6(b). On the other hand, the developed controller, is capable of dealing with the impacts of these nonlinearities while maintaining system stability.

Figure 5 Power system with GDB and GRC (see online version for colours)

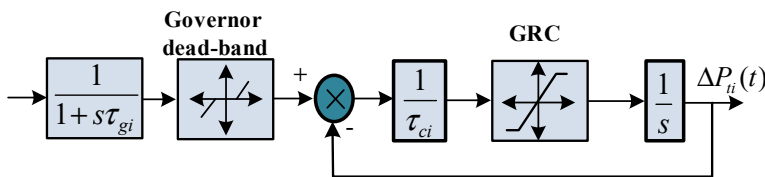
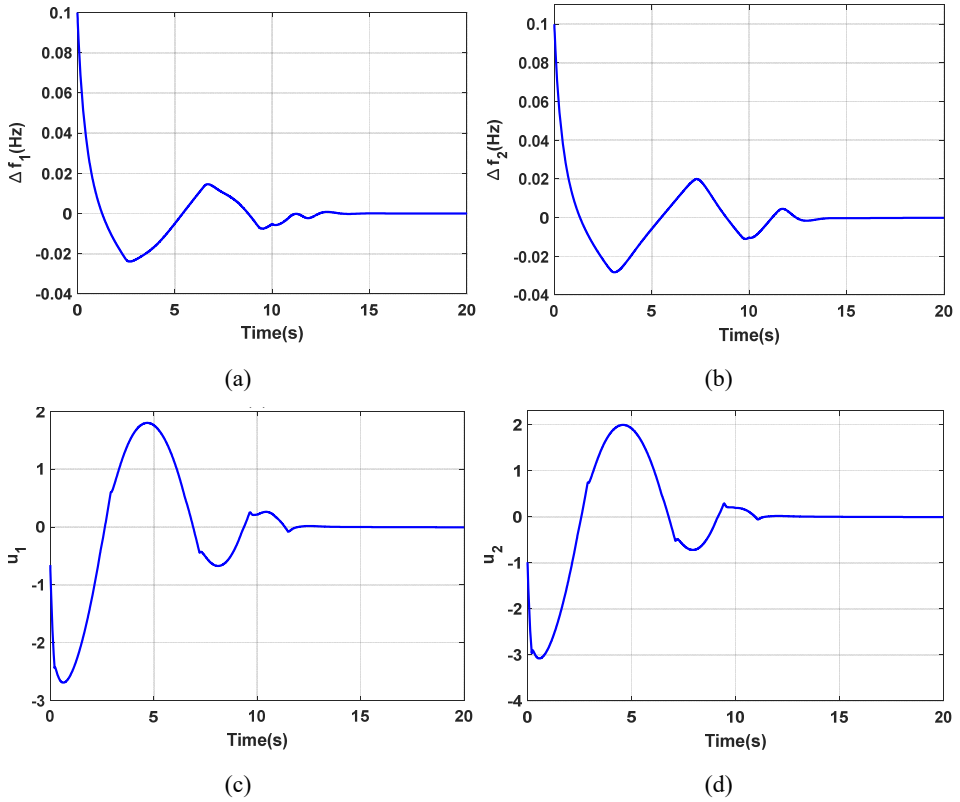


Figure 6 (a) FD in area-1 (b) FD in area-2 (c) CI in area-1 (d) CI in area-2 (see online version for colours)



Case 4

To carry out the analysis on a realistic platform, the system dynamics has been assessed for multi-sources such as wind turbine generator (WTG), battery energy storage (BES), and diesel engine generator (DEG) with 5% load disturbance in time-delayed IPS, as illustrated in Figure 7. The model of WTG is considered from Patel et al. (2021). The IST-ISMC is applied in the variable speed WTG to regulate the output power of wind system. In this case, a variable wind speed [Figure 8(a)] WTG connected in area-1, BES in area-2, DEG in area-2, and load disturbance are simultaneously applied to time-delayed IPS (Figure 7). The dynamic performance of this power system model with these perturbations is plotted in Figure 8. It is apparent from Figures 8(b)–8(f) that the FD with proposed IST-ISMC is minimum and can speedily attain the steady-state value.

Figure 7 Multi-source two-area IPS model with RFB (see online version for colours)

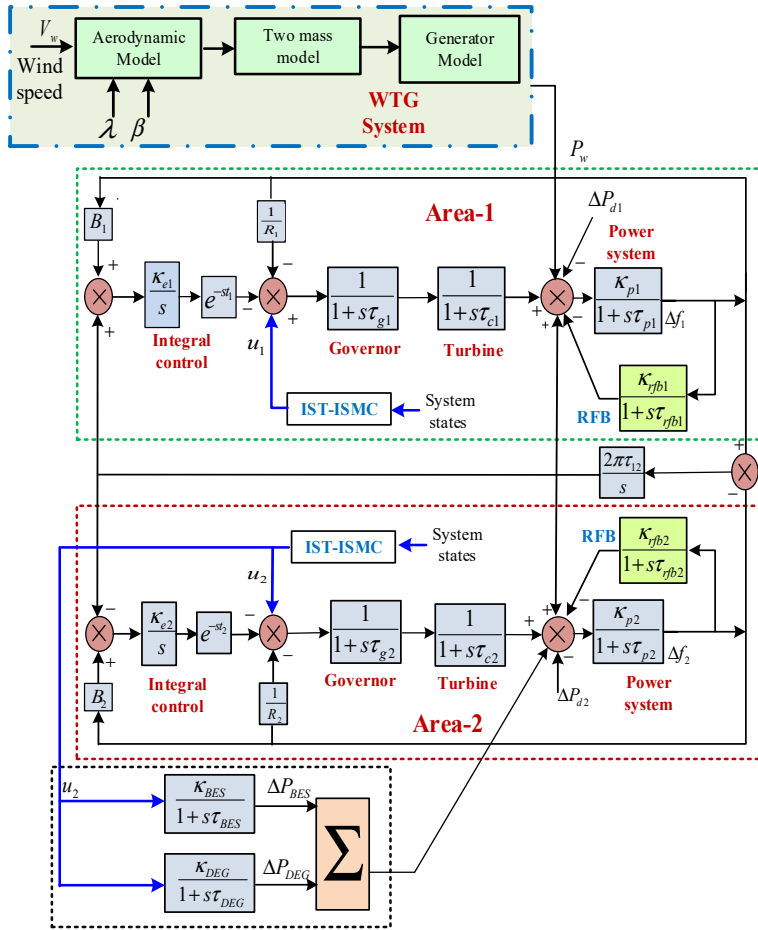


Figure 8 (a) Wind speed (b) Output of BESS (c) Output of DEG (d) FD in area-1 (e) FD in area-2 (f) T-LPD (see online version for colours)

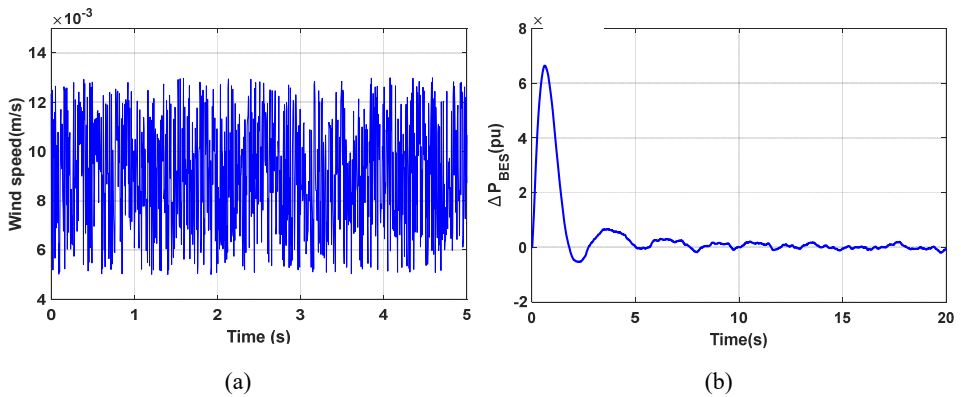
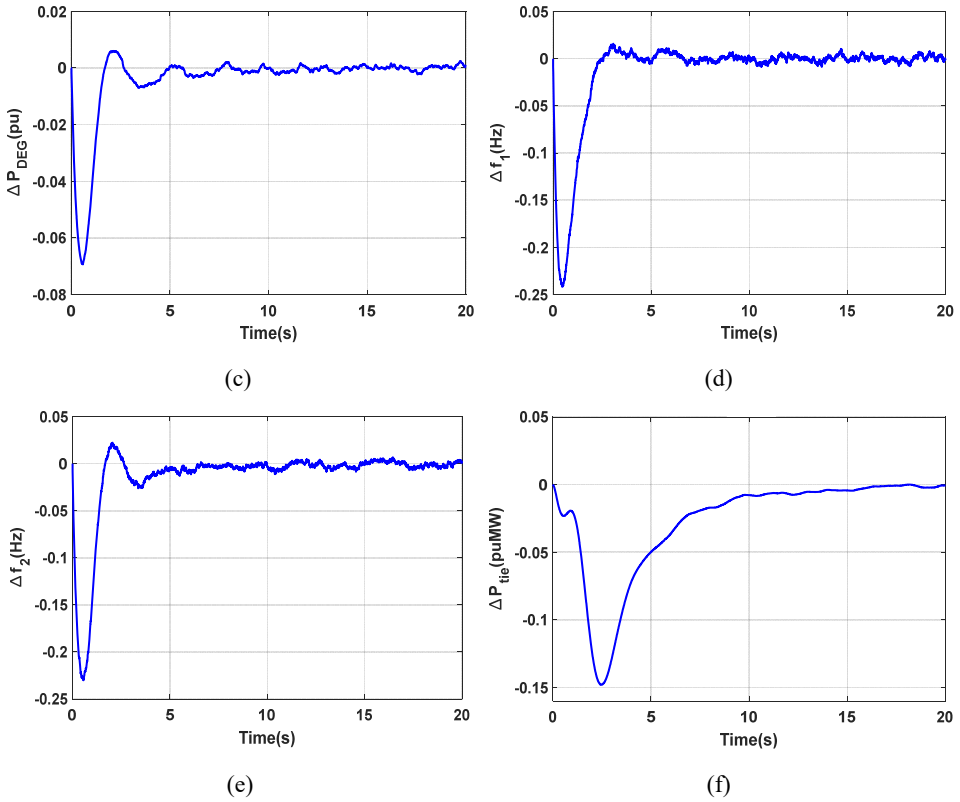


Figure 8 (a) Wind speed (b) Output of BESS (c) Output of DEG (d) FD in area-1 (e) FD in area-2 (f) T-LPD (continued) (see online version for colours)



5 Conclusions

The effect of time-delay and RFB on frequency regulation of IPS has been studied in this paper. An improved super twisting integral sliding mode controller (IST-ISMC) is built for frequency regulation of time-delay IPS with RFB. In IST-ISMC, a new reaching law is used which results in fast convergence while minimising the chattering phenomenon. The IST-ISMC produces better results than ISMC (Sun et al., 2018) in terms of convergence and chattering in the controller output as is evident from simulation results.

RFBs are added to both the areas of IPS to improve the overall response of the system. As a result, the IST-ISMC controllers with an RFB outperform the IST-ISMC controller without an RFB in terms of settling time, peak overshoot and undershoot. To assess the robustness of the proposed control technique, the effects of inherent power system nonlinearities such as GRC and GDB, as well as wind power penetrations, BES, DEG on system outputs were investigated.

References

- Akbar, R. and Uchiyama, N. (2017) 'Adaptive modified super-twisting control for a quadrotor helicopter with a nonlinear sliding surface', *2017 SICE International Symposium on Control Systems (SICE ISCS)*, pp.1–6.
- Akbar, R. and Uchiyama, N. (2018) 'Design and experiment of adaptive modified super-twisting control with a nonlinear sliding surface for a quadrotor helicopter', *Advances in Mechanical Engineering*, Vol. 10, No. 10, pp.1–19.
- Arya, Y. and Kumar, N. (2016) 'Fuzzy gain scheduling controllers for automatic generation control of two-area interconnected electrical power systems', *Electric Power Components and Systems*, Vol. 44, No. 7, pp.737–751.
- Arya, Y., Kumar, N. and Ibraheem (2015) 'AGC of a two-area multi-source power system interconnected via AC/DC parallel links under restructured power environment', *Optimal Control Applications and Methods*, Vol. 37, No. 4, pp.590–607.
- Bevrani, H. and Hiyama, T. (2008) 'Robust decentralized PI based LFC design for time delay power systems', *Energy Conversion and Management*, Vol. 49, No. 7, pp.93–204.
- Bevrani, H., Mitani, Y. and Tsuji, K. (2004) 'Robust decentralised load frequency control using an iterative linear matrix inequalities algorithm', *IEE Proceedings – Generation, Transmission and Distribution*, Vol. 151, pp.347–354.
- Daneshfar, F. and Bevrani, H. (2012) 'Multiobjective design of load frequency control using genetic algorithms', *International Journal of Electrical Power & Energy Systems*, Vol. 42, No. 1, pp.257–263.
- Dev, A., Léchappé, V. and Sarkar, M.K. (2021) 'Prediction-based super twisting sliding mode load frequency control for multi-area interconnected power systems with state and input time delays using disturbance observer', *International Journal of Control*, Vol. 94, No. 7, pp.1751–1764.
- Dey, R., Ghosh, S., Ray, G. and Rakshit, A. (2012) 'H ∞ load frequency control of interconnected power systems with communication delays', *International Journal of Electrical Power & Energy Systems*, Vol. 42, No. 1, pp.672–684.
- Dhandapani, L., Abdulkareem, P. and Muthu, R. (2018) 'Two-area load frequency control with redox flow battery using intelligent algorithms in a restructured scenario', *Turkish Journal of Electrical Engineering & Computer Sciences*, Vol. 26, No. 1, pp.330–346.
- Gorripotu, T.S., Kumar, D.V., Boddepalli, M.K. and Pilla, R. (2018) 'Design and analysis of BFOA optimised PID controller with derivative filter for frequency regulation in distributed generation system', *International Journal of Automation and Control*, Vol. 12, No. 2, pp.291–323.
- Guo, J. and Dong, L. (2017) 'Robust load frequency control for uncertain nonlinear interconnected power systems', *International Journal of Automation and Control*, Vol. 11, No. 3, pp.239–261.
- Heshmati, M., Noroozian, R., Jalilzadeh, S. and Shayeghi, H. (2020) 'Optimal design of CDM controller to frequency control of a realistic power system equipped with storage devices using grasshopper optimization algorithm', *ISA Transactions*, Vol. 97, pp.202–215, <https://doi.org/10.1016/j.isatra.2019.08.028>.
- Hussein, A.A., Hasan, N., Nasirudin, I. and Farooq, S. (2020) 'Load frequency controller for multisource interconnected nonlinear power system incorporating FACTS devices', *International Journal of Automation and Control*, Vol. 4, No. 3, pp.257–283.
- Jagatheesan, K., Anand, B., Dey, N., Ashour, A.S. and Balas, V.E. (2018) 'Load frequency control of multi-area interconnected thermal power system: artificial intelligence-based approach', *International Journal of Automation and Control*, Vol. 12, No. 1, pp.126–152.
- Jiang, L., Yao, W., Wu, Q.H., Wen, J.Y. and Cheng, S.J. (2012) 'Delay dependent stability for load frequency control with constant and time-varying delays', *IEEE Transactions on Power Systems*, Vol. 27, No. 2, pp.932–941.

- Ju, P., Handschin, E. and Karlsson, D. (1996) 'Nonlinear dynamic load modelling: model and parameter estimation', *IEEE Transactions on Power Systems*, Vol. 11, No. 4, pp.1689–1697.
- Kumar, A. and Pan, S. (2021) 'Design of fractional order PID controller for load frequency control system with communication delay', *ISA Transactions*, Vol. 129, Part A, pp.138–149, <https://doi.org/10.1016/j.isatra.2021.12.033>.
- Kumar, S.R. and Ganapathy, S. (2016) 'Impact of energy storage units on load frequency control of deregulated power systems', *Energy*, Vol. 97, pp.214–228, <https://doi.org/10.1016/j.energy.2015.12.121>.
- Lim, K.Y., Wang, Y. and Zhou, R. (1996) 'Robust decentralised load-frequency control of multi-area power systems', *IEE Proceedings – Generation, Transmission and Distribution*, Vol. 143, No. 5, pp.377–386.
- Mi, Y., Fu, Y., Wang, C. and Wang, P. (2013) 'Decentralized sliding mode load frequency control for multi-area power systems', *IEEE Transactions on Power Systems*, Vol. 28, No. 4, pp.4301–4309, DOI: 10.1109/TPWRS.2013.2277131.
- Muthana, T.A. and Mohamed, Z. (2013) 'On the control of time delay power systems', *International Journal of Innovative Computing, Information and Control*, Vol. 9, No. 2, pp.769–792.
- Pappachen, A. and Fathima, A.P. (2016) 'Load frequency control in deregulated power system integrated with SMES-TCPS combination using ANFIS controller', *International Journal of Electrical Power & Energy Systems*, Vol. 82, pp.19–534, DOI: 10.1016/j.ijepes.2016.04.032.
- Patel, V., Guha, D. and Purwar, S. (2021) 'Neural network aided fractional-order sliding mode controller for frequency regulation of nonlinear power systems', *Computers & Electrical Engineering*, Vol. 96, p.107534, <https://doi.org/10.1016/j.compeleceng.2021.107534>.
- PeerFathima, L.A. and Ranganath, M. (2018) 'Two-area load frequency control with redox flow battery using intelligent algorithms in a restructured scenario', *Turkish Journal of Electrical Engineering & Computer Sciences*, Vol. 26, No. 1, pp.330–346.
- Pradhan, S.K. and Das, A.D.K. (2020) 'Robust H_{∞} sliding mode control design for wind-integrated interconnected power system with time-delay and actuator saturation', *Grids and Networks: Sustainable Energy*, Vol. 23, p.100370, <https://doi.org/10.1016/j.compeleceng.2021.107534>.
- Prasad, S., Purwar, S. and Kishor, N. (2016) 'H-infinity based non-linear sliding mode controller for frequency regulation in interconnected power systems with constant and time-varying delays', *IET Generation, Transmission & Distribution*, Vol. 10, No. 11, pp.2771–2784.
- Saxena, S. and Hote, Y.V. (2016) 'Decentralized PID load frequency control for perturbed multi-area power systems', *International Journal of Electrical Power & Energy Systems*, Vol. 81, pp.405–415, <https://doi.org/10.1016/j.ijepes.2016.02.041>.
- Sharma, G., Krishnan, N., Arya, Y. and Panwar, A. (2021a) 'Impact of ultracapacitor and redox flow battery with JAYA optimization for frequency stabilization in linked photovoltaic-thermal system', *International Journal of Electrical Power & Energy Systems*, Vol. 31, No. 5, p.e12883.
- Sharma, M., Dhundhara, S., Arya, Y. and Prakash, S. (2021b) 'Frequency stabilization in deregulated energy system using coordinated operation of fuzzy controller and redox flow battery', *International Journal of Energy Research*, Vol. 45, No. 5, pp.7457–7475.
- Sharma, M., Dhundhara, S., Arya, Y. and Prakash, S. (2020) 'Frequency excursion mitigation strategy using a novel COA optimised fuzzy controller in wind integrated power systems', *IET Renewable Power Generation*, Vol. 14, No. 19, pp.4071–4085.
- Sheirah, M.A. and Abd-El-Fattah, M.M. (1984) 'Improved load-frequency self-tuning regulator', *International Journal of Control*, Vol. 39, No. 1, pp.143–158.
- Sudha, K.R. and Santhi, R.V. (2011) 'Robust decentralized load frequency control of interconnected power system with generation rate constraint using type-2 fuzzy approach', *International Journal of Electrical Power & Energy Systems*, Vol. 33, No. 3, pp.699–707.

- Sun, Y., Wang, Y., Wei, Z., Sun, G. and Wu, X. (2018) ‘Robust H_∞ load frequency control of multi-area power system with time delay: a sliding mode control approach’, *IEEE/CAA Journal of Automatica Sinica*, Vol. 5, No. 2, pp.610–661.
- Utkin, V. (1977) ‘Variable structure systems with sliding modes’, *IEEE Transactions on Automatic Control*, Vol. 22, No. 2, pp.212–222.
- Xia, Y.Q. and Jia, Y.M. (2003) ‘Robust sliding-mode control for uncertain time-delay systems: an LMI approach’, *IEEE Transactions on Automatic Control*, Vol. 48, No. 6, pp.1076–1091.
- Yu, X.F. and Tomsovic, K. (2004) ‘Application of linear matrix inequalities for load frequency control with communication delays’, *IEEE Transactions on Power Systems*, Vol. 19, No. 3, pp.1508–1515.
- Zhang, C.K., Jiang, L., Wu, Q.H., He, Y. and Wu, M. (2013) ‘Delay-dependent robust load frequency control for time delay power systems’, *IEEE Transactions on Power Systems*, Vol. 28, No. 3, pp.2192–2201.

Appendix

- Nominal parameter of IPS (Sun et al., 2018)

$\kappa_{p1} = 1$	$\tau_{p1} = 10$	$\tau_{c1} = 0.3$	$\tau_{g1} = 0.1$	$B_1 = 41$	$R_1 = 0.05$	$K_{e1} = 0.5$
$\kappa_{p2} = 0.67$	$\tau_{p2} = 8$	$\tau_{c2} = 0.17$	$\tau_{g2} = 0.4$	$B_1 = 81.5$	$R_2 = 0.05$	$K_{e2} = 0.5$

- Parameters of RFB (Dhandapani et al., 2018)

$$\kappa_{rfb} = 1.8, \tau_{rfb} = 0$$

- Parameters of DEG

$$\kappa_{DEG} = 2.3, \tau_{DEG} = 0.3$$

- Parameters of BES

$$\kappa_{BES} = 0.003, \tau_{BES} = 0.1$$

- Controller parameter

$$\kappa_1 = \begin{bmatrix} 6.93 & 5.40 & -5.38 & -40.83 & -5.58 & -8.73 & 0.47 & 1.10 & 23.64 \\ 8.65 & 6.42 & -5.73 & -45.41 & -5.18 & -10.09 & -1.87 & 2.76 & 25.94 \end{bmatrix}$$

$$\kappa_2 = \begin{bmatrix} 10 & -0.1 & 0 & 0 & 0 & 0 & 0 & 0 & 0 \\ 0 & 0 & 0 & 0 & 0 & 12 & 0 & 0.4 & 0 \end{bmatrix}$$

$$\kappa_x = \text{diag}(0.1 \quad 0.2)$$

$$\kappa_y = \text{diag}(0.05 \quad 0.1)$$

$$\kappa_z = \text{diag}(0.5 \quad 0.1).$$